Preprint submitted to Computational Mechanics manuscript No.
(will be inserted by the editor)

Space-Time Finite Element Methods for Dynamic Frictional Contact Problems

Andreas Rademacher

Received: date / Accepted: date

Abstract Space-time finite element methods for dynamic frictional contact problems are discussed in this article. The discretization scheme is based on a mixed formulation of the continuous problem, where the Lagrange multipliers represent the contact and frictional stresses. Using piecewise d-linear and globally continuous basis functions in space and time to construct the trial space for the displacement as well as the velocity field and combining it with a test space consisting of piecewise constant and possibly discontinuous basis functions in time, a space-time Galerkin method is constructed. The Lagrange multipliers are approximated by piecewise constant functions in space and time. Several methods to ensure the stability of the Lagrange multipliers are proposed and compared numerically.

Keywords Dynamic contact problems · Friction · Space-time finite element method · Mixed method

1 Introduction

Dynamic contact problems with friction play an important role in many engineering processes. We exemplify milling and grinding processes here. The contact of the tool and the workspiece is typically the main source of dynamic deflections of the metal-cutting machine, where the contact arises only in a small area. Consequently, it is essential in the simulation of such processes to use an accurate and reliable numerical scheme to approximate the contact. We refer to [1] for an elaborated description of a grinding process and the corresponding simulation approach.

A. Rademacher
Institute of Applied Mathematics, Technische Universität Dortmund, D-44221 Dortmund, Germany
E-mail: andreas.rademacher@mathematik.tu-dortmund.de

The inclusion of geometrical and frictional constraints lead to inequality conditions in addition to the usual systems of partial differential equations arising from the modeling of mechanical processes, c.f. [2–4]. The numerical solution of dynamic contact problems is a challenging task and a huge number of approaches are presented in literature. We refer to the monographs [3, 4] and the survey articles [5,6] for an overview. Usually, finite difference schemes are used for the discretization of the temporal direction and finite element methods are applied for the approximation of the spatial problems. In general Rothe's method is employed, i.e. the temporal variable is discretized first. Using special parameters in the Newmark [7] or in the generalized-α method [8], discretization schemes for dynamic contact problems are proposed in [9–11]. An important topic during the discretization is the conservation of energy and momentum. Discretization methods based on these conservation properties are developed in [12,13]. A second crucial issue are arising oscillations in the contact forces. One approach to circumvent these oscillations but preserving energy conservation is to redistribute the mass in the system by changing the mass matrix. In [14], the mass matrix is modified by optimization algorithms, whereas special quadrature rules are used in [15]. An complete implicit treatment of the contact constraint is implemented in the Newmark method in [16, 17]. This scheme is stable but energy dissipative. Using a modified predictor step in the Newmark method, an L^2-projection of the predicted displacement onto the admissible set, a stable scheme is introduced in [18,19], which is only slightly energy dissipative. Furthermore, a consistency result and an adaptive time stepping for this method is presented in [20–22]. Space adaptive discretizations are discussed in [23,24]. A penalty method to solve dynamic contact problems is developed in [25].

Special finite elements to smooth the contact forces are applied in [26,27].

The time discretization leads to a sequence of semi-discrete contact problems, which are similar to static contact problems. Consequently, the same solution techniques are applied. Also for the numerical solution of static contact problems, a huge number of contributions exist. Again, we refer to the monographs [3,4]. This field of research is still an important subject and we refer to the recent works [28–32]. We employ the techniques developed in [33–36] and extended to higher order finite elements in [37,38].

In this article, we focus on the holistic discretization of dynamic contact problems, i.e. the temporal and spatial discretization is carried out simultaneously. This approach allows for the consideration of space-time effects in a simpler way. Thus, the analysis of the approach is simpler and provides more insight into the interaction of space and time. We refer to [39] for a posteriori error analysis and adaptive methods. Our approach relies on a mixed formulation in space-time, which is elaborately explained in Section 2, where we compare it to the strong formulation and the formulation as variational inequality. After the introduction of the continuous problem formulation, we present the low order finite element scheme in more details. Piecewise d-linear and globally continuous basis functions in space and time are used to form the trial space for the displacement and the velocity. The corresponding test space consists of piecewise constant and discontinuous basis functions in time and piecewise d-linear and globally continuous basis functions in space. The Lagrange multipliers are discretized by piecewise constant and discontinuous basis functions in space and time. In Section 3, we proof that this approach is energy conserving. The choice of a discontinuous test space is crucial for this discretization, because it enables us to decouple the single time intervals and to derive a time stepping scheme, c.f. Section 4. The arising discrete problem in every time step is simplified concerning the side conditions to ease the calculation. Due to this, the scheme fulfills the side conditions w.r.t. to the displacement only approximately and we obtain energy conservation on temporal patches only, not in the interior. Finally, we present a reformulation of the discrete problem as quadratic program with box constraints in each time step. To ensure the stability of the approach, we have to define the Lagrange multipliers on coarser meshes in space and time. This is a generalization of the results presented in [37] to the time dependent case. We substantiate the stability by numerical examples in Section 5. Unfortunately, a second assumption for stability is found, which corrolates the spatial mesh width with the time step length similar to CFL conditions. We discuss three other ways to stabilize the discretization in time without coarsening the temporal mesh for the Lagrange multipliers. The first idea is to use the right box rule for integrating some temporal integrals with less accuracy than originally required. What we recover is a discretization scheme, which corresponds to a piecewise constant and discontinuous approximation of the velocity. It is stable, but strongly numerically dissipative and converges only of first order for unconstrained problems in comparison to the convergence of second order of the original scheme. Consequently, we discourage the use of it. An other tested approach is to redistribute the mass in the mass matrix using the ideas discussed in [15]. This scheme works quite nice just like the fourth approach. It is based on an additional projection of the velocity onto the admissible set and is similar to the one in [18]. The scheme is stable but weakly energy dissipative. All in all, we provide three reasonable approximation schemes of the original Galerkin solution, which can be interpreted as some sort of variational crime. The findings are substantiated by the numerical results in Section 6, which show the applicabilty of the approaches. Furthermore, the approaches are compared w.r.t. accuracy and energy conservation. We conclude the paper with a discussion of the results and an outlook on further tasks.

2 Continuous Formulation

In this section, we discuss the continuous formulation of the dynamic frictional contact problem. The initial point is the strong formulation, which is reformulated in the weak sense as variational inequality and then as mixed problem. The mixed formulation is the basis for the presented discretisation. The section concludes with some remarks on the analytic properties of the dynamic frictional contact problem. In the presentation, we restrict ourselves to Signorini's problem, i.e. we consider an elastic body in contact with a rigid obstacle. This is only done to simplify the notations. The presented discretisation directly carries over to multibody contact problems. It requires just the usual changes in the spatial discretisation.

2.1 Strong formulation

The basic domain is $\Omega \subset \mathbb{R}^d$, $d = 2, 3$ and $I = [0, T]$ the time interval. The boundary $\partial\Omega$ of Ω is divided into three mutually disjoint parts Γ_D, Γ_C and Γ_N with positive measure. Homogeneous Dirichlet and Neumann boundary conditions are prescribed on the closed set

Γ_D and on the relatively open set Γ_N, respectively. Contact may take place on the sufficiently smooth set Γ_C, $\bar{\Gamma}_C \subset \complement\Gamma_D$. See, for instance, [2], Section 5.3, for more details. The rigid foundation is parametrized by the function $g : \Gamma_C \to \mathbb{R} \cup \{-\infty\}$ including a suitable linearization, cf. [2]. The obstacle is assumed to be constant in time to simplify the notations. However, all results carry over to time depending obstacles.

In the description of dynamic contact problems, we assume homogeneous Neumann boundary conditions to ease the notation. A linear elastic material model is used to describe the material behaviour. The displacement is given by the function $u : \Omega \times I \to \mathbb{R}^d$ and u_n is the displacement on the boundary in the outward normal direction. In this context, $\varepsilon(u) := \frac{1}{2}\left(\nabla u + \nabla u^\top\right)$ denotes the strain and $\sigma(u) = \mathbb{C}\varepsilon(u)$ the stress. The fourth order tensor $\mathbb{C}$ only depends on the modulus of elasticity $E > 0$ and Poisson's ratio $\nu \in \left[0, \frac{1}{2}\right)$. By $\sigma_n(u)$, we denote the stress on the surface, where we distinguish between $\sigma_{nn}(u)$, the stress on the surface in normal direction, and $\sigma_{nt}(u)$, the stress in tangential direction. Superposed dots denote temporal derivatives.

If the solution u is sufficiently smooth, for instance $u \in C^2(\Omega \times I)$, it fulfils the equations of structural dynamics including the boundary and initial conditions

$$\ddot{u} - \operatorname{div}(\sigma(u)) = f \quad \text{in } \Omega \times I, \tag{1}$$
$$u = 0 \quad \text{on } \Gamma_D \times I, \tag{2}$$
$$\sigma_n(u) = 0 \quad \text{on } \Gamma_N \times I, \tag{3}$$
$$u(0) = u_s \quad \text{in } \Omega, \tag{4}$$
$$\dot{u}(0) = v_s \quad \text{in } \Omega, \tag{5}$$

the contact conditions

$$u_n - g \le 0 \quad \text{on } \Gamma_C \times I, \tag{6}$$
$$\sigma_n(u) \le 0 \quad \text{on } \Gamma_C \times I, \tag{7}$$
$$\sigma_{nn}(u)(u_n - g) = 0 \quad \text{on } \Gamma_C \times I, \tag{8}$$
$$\sigma_{nn}(u)\,\dot{u}_n = 0 \quad \text{on } \Gamma_C \times I, \tag{9}$$

as well as the frictional conditions on $\Gamma_C \times I$

$$|\sigma_{nt}(u)| \le s, \tag{10}$$
$$|\sigma_{nt}(u)| < s \Rightarrow \dot{u}_t = 0, \tag{11}$$
$$|\sigma_{nt}(u)| = s \Rightarrow \exists \zeta > 0 : \dot{u}_t = -\zeta \sigma_{nt}. \tag{12}$$

Henceforth, we set $\rho \equiv 1$ for notational simplicity. In comparison to the static contact case, the persistency condition (9) has been added. It corresponds to the complementarity condition (8), only the gap $u_n - g$ is replaced by the gap rate $\dot{u}_n$. In Proposition 1, we see that the persistency condition ensures the conservation of energy, if no outer forces and no friction occurs. Therewith, the impact is purely elastic. To clarify the physical meaning of the persistency condition, we examine the following equivalent form (c.f. [3]) of the contact conditions (6-9) on $\Gamma_C \times I$:

$$u_n - g < 0 \Rightarrow \sigma_{nn}(u) = 0,\ \dot{u}_n \text{ unconstrained}, \tag{13}$$
$$u_n - g = 0 \Rightarrow \sigma_{nn}(u) \le 0,\ \dot{u}_n \le 0,\ \sigma_{nn}\dot{u}_n = 0. \tag{14}$$

The condition (13) says that the movement of the elastic body is free, if the gap is open. If the gap is closed, then condition (14) denotes that the contact stresses are negative, which is known from the static context. But now, the velocity has to be less than zero, too. This ensures that $u_n - g \le 0$ holds. Furthermore, we recover the persistency condition (9). We will use a discrete version of (13-14) to enforce the contact conditions in our numerical calculations.

The conditions (10-12) describe Tresca friction where the frictional resistance is given by the function $s \ge 0$. Here, an index t denotes the velocity in tangential direction on the boundary. If the tangential stress is smaller than s, then the tangential velocity is zero, otherwise the tangential velocity is proportional to σ_{nt}. The choice $s = \mathcal{F}|\sigma_{nn}|$ with an coefficient $\mathcal{F} \ge 0$ leads to Coulomb's law of friction.

2.2 Weak formulation

After having discussed the strong formulation, we now define the weak one. To this end, we briefly present the underlying function spaces. A detailed description can be found for instance in [2,40].

The basic function space is $L^2(\Omega)$ with scalar product (ω, φ) for $\omega, \varphi \in L^2(\Omega)$ and the corresponding norm is $\|\omega\|_0$. The Sobolev space $H^k(\Omega)$, $k = 1, 2, \ldots$, with the norm $\|\cdot\|_k^2$ is defined as usual. We set $\mathcal{H}^k := \left(H^k(\Omega)\right)^d$ and $\mathcal{L}^2 := \left(L^2(\Omega)\right)^d$. The trace operator is given by $\gamma : \mathcal{H}^1 \to \left(L^2(\partial\Omega)\right)^d$. Here, we distinguish between the trace in normal direction $\gamma_n(u) := \left(\gamma_{|\Gamma_C}(u)\right)_n$ and the one in tangential direction $\gamma_t(u) := \left(\gamma_{|\Gamma_C}(u)\right)_t$. The Hilbert space $H^{1/2}(\partial\Omega)$ with the usual norm $\|\cdot\|_{1/2}$ is dense in $L^2(\partial\Omega)$. The dual space of $H^{1/2}(\partial\Omega)$ is $H^{-1/2}(\partial\Omega)$ with the norm $\|\cdot\|_{-1/2}$.

Using the trace operator, we define

$$H^1(\Omega, \Gamma_D) := \left\{\varphi \in H^1(\Omega) \,|\, \gamma_{|\Gamma_D}(\varphi) = 0\right\},$$

$\mathcal{H}^1_D := \left(H^1(\Omega, \Gamma_D)\right)^d$. The dual space $\left(H^1(\Omega, \Gamma_D)\right)^\star$ is called $H^{-1}(\Omega)$ and $\left(\mathcal{H}^1_D\right)^\star = \mathcal{H}^{-1}$. The dual pairing is denoted by $\langle \cdot, \cdot \rangle$.

We define the space $H^{1/2}(\Gamma_C)$ as usual. It is a closed subspace of $H^{1/2}(\partial\Omega)$ and thus a Hilbert space provided with the associated norm $\|\cdot\|_{1/2,\Gamma_c}$. The space $H^{-1/2}(\Gamma_C)$ is the dual space of $H^{1/2}(\Gamma_C)$. The norm connected to $H^{-1/2}(\Gamma_C)$ is called $\|\cdot\|_{-1/2,\Gamma_C}$.

Using the Bochner integral theory, we can study Sobolev spaces involving time. We employ the spaces $L^p(I;X)$, $1 \leq p \leq \infty$, with a real Banach space X. Continuous functions in time form the space $C(I;X)$. If X is a Hilbert space with scalar product $(\cdot,\cdot)$, then the space-time scalar product is denoted by $((u,v)) := \int_I (u(t),v(t))\,dt$. In general, an outer parenthesis denotes the integration over I.

Finally, we are able to define a weak solution of the dynamic contact problem:

Definition 1 A function $u \in K$ is a weak solution of the dynamic contact problem if and only if

$$\begin{aligned}\langle \ddot{u}, \varphi - \dot{u}\rangle + a(u, \varphi - \dot{u}) \\ +j(\varphi) - j(\dot{u}) \geq (f, \varphi - \dot{u}) \quad (15)\\ (\sigma_{nn}(u), \gamma_n(\dot{u}))_{\Gamma_C} = 0 \quad (16)\\ u(0) = u_s \quad (17)\\ \dot{u}(0) = v_s \quad (18)\end{aligned}$$

holds for all $\varphi \in \tilde{K}$ and a.e. time $t \in I$ with

$$\begin{aligned}W &:= \left\{ \varphi \in L^2\left(I;\mathcal{H}^1_D\right) \,\middle|\, \begin{array}{l}\dot{\varphi} \in L^2\left(I;\mathcal{H}^1_D\right),\\ \ddot{\varphi} \in L^2\left(I;\mathcal{H}^{-1}\right)\end{array} \right\},\\ K &:= \{\varphi \in W \,|\gamma_n(\varphi)(t,x) \leq g(x) \text{ a.e. } t \in I,\, x \in \Gamma_C\},\\ \tilde{K} &:= \left\{\varphi \in \mathcal{H}^1_D \,|\gamma_n(\varphi)(x) \leq g(x) \text{ a.e. } x \in \Gamma_C\right\}.\end{aligned}$$

Furthermore, $f \in L^2\left(I;\mathcal{L}^2\right)$, $u_s \in \mathcal{H}^1_D$, and $v_s \in \mathcal{L}^2$.

The bilinear form a is given by $a(\cdot,\cdot) := (\sigma(\cdot), \varepsilon(\cdot))$. It is continuous and also elliptic due to Korn's inequality. The functional j representing the frictional forces is specified by $j(\varphi) := (s, |\gamma_t(\dot{u})|)_{\Gamma_C}$. If the solution u is sufficiently smooth, (15) and (17-18) are equivalent to (1-8), see for instance [9]. The generalised persistency condition (16) (c.f. [20]) corresponds to the pointwise persistency condition (9) due to the sign conditions in (13-14).

It should be remarked that the existence and uniqueness of a solution u for the purely elastic dynamic Signorini problem is an open question. In [41], the existence of a weak solution has been shown for the viscoelastic Signorini problem.

Since the mixed formulation of the dynamic contact problem is more suited for the analysis of the problem and for the discretisation, we rewrite the variational inequality (15) in the mixed form:

Definition 2 The functions $(w,\lambda) \in (U \times V) \times \Lambda$ with $w = (u,v)$, $\lambda = (\lambda_n, \lambda_t)$, and $\Lambda = \Lambda_n \times \Lambda_t$ are a weak solution of the dynamic contact problem, if and only if there holds

$$\begin{aligned}A(w,\varphi) + (b(\lambda,\chi,\chi)) = 0, \quad (19)\\ b(\mu - \lambda, u - g, \dot{u}) \leq 0,\\ \langle \lambda_n, \gamma_n(\dot{u})\rangle = 0, \quad (20)\end{aligned}$$

for all $\varphi = (\psi,\chi) \in U \times V$, all $\mu \in \bar{\Lambda}$, and a.e. $t \in I$.

We have rewritten the problem in terms of the displacement u and the velocity v. Furthermore, inequality (15) has been integrated over the time interval I. Thus, we end up with a space-time formulation.

The trial spaces for the displacement and the velocity are

$$\begin{aligned}U &:= \left\{\psi \in L^2\left(I;\mathcal{H}^1\right) \,\middle|\, \dot{\psi} \in L^2\left(I;\mathcal{H}^1\right)\right\},\\ V &:= \left\{\chi \in L^2\left(I;\mathcal{H}^1\right) \,\middle|\, \dot{\chi} \in L^2\left(I;\mathcal{L}^2\right)\right\}.\end{aligned}$$

The definition of Λ is more involved. First, we introduce the spatial sets

$$\begin{aligned}G_n &:= \left\{\mu \in H^{1/2}(\Gamma_C) \,\middle|\, \mu \leq 0\right\}^\star,\\ G_t &:= \left\{\mu \in \left(L^2(\Gamma_C)\right)^{d-1} \,\middle|\, \begin{array}{l}|\mu| \leq 1 \text{ on } \operatorname{supp}(s),\\ \mu = 0 \text{ on } \Gamma_C \backslash \operatorname{supp}(s)\end{array}\right\}.\end{aligned}$$

The Lagrange multiplier is assumed to be in L^2 in time and consequently we set $\Lambda_n := L^2(I;G_n)$ and $\Lambda_t := L^2(I;G_t)$. Furthermore, we define $\bar{\Lambda} := G_n \times G_t$.

The space-time bilinear form A is given by

$$\begin{aligned}A(w,\varphi) := ((v - \dot{u}, \psi)) + ((\dot{v},\chi)) + (a(u,\chi)) - ((f,\chi))\\ + (u(0) - u_s, \chi(0)) + (v(0) - v_s, \psi(0)),\end{aligned}$$

where the first term expresses the weak equality of v and $\dot{u}$ and the terms in the second line weakly enforce the initial conditions. The form

$$b(\lambda,\varphi,\chi) := \langle \lambda_n, \gamma_n(\varphi)\rangle + (\lambda_t, s\gamma_t(\chi))_{\Gamma_C}$$

represents the contact- and frictional conditions.

The mixed formulation and its equivalence to the variational inequality formulation are discussed, e.g., in [12,42]. In particular, the equality of σ_{nn} and λ_n is considered. Now, we examine the energy conservation:

Proposition 1 *If the right hand side f is zero and no friction occurs the total energy is conserved in the dynamic contact problem.*

Proof We test equation (19) by $(\dot{v},\dot{u})$ and obtain

$$\begin{aligned}0 &= ((\dot{v},v)) + (a(u,\dot{u})) + \left(\left\langle \lambda_n, \gamma_{|\Gamma_C,n}(\dot{u})\right\rangle\right)\\ &= \frac{1}{2}\left(\frac{\partial}{\partial t}(v,v) + \frac{\partial}{\partial t}a(u,u)\right) + \left(\left\langle \lambda_n, \gamma_{|\Gamma_C,n}(\dot{u})\right\rangle\right).\end{aligned}$$

Hence, the temporal derivative of the total energy is given by

$$\int_I \frac{\partial}{\partial t} E_{tot}\,dt = -\left(\left\langle \lambda_n, \gamma_{|\Gamma_C,n}(\dot{u})\right\rangle\right).$$

Because of condition (20), the term on the right hand side vanishes and therewith, the total energy is conserved. Using more complex test functions, we can also show that the total energy is constant.

Remark 1 The linear and the angular momentum are also conserved under suitable assumptions, see for instance [3].

3 Discretization

In this section, we discuss the discretisation scheme and show some properties of it. The chosen ansatz is a Petrov-Galerkin scheme, with continuous and piecewise linear basis functions in time for the displacement and the velocity. We call it cG(1)cG(1) method. The Lagrange multiplier is discretised with piecewise constant and discontinuous functions in space and time. As usual in mixed methods, special attention has to be paid to the balancing of the discretisation of the primal and the dual variable.

The temporal discretisation is based on a decomposition of the time interval $I = [0, T]$ into $M \in \mathbb{N}$, M even, subintervals $I_m = (t_{m-1}, t_m]$ with $I_0 = \{0\}$, $0 = t_0 < t_1 < \ldots < t_M = T$, and $I = \bigcup_{m=0}^{M} I_m$. The length of a subinterval I_m is $k_m := t_m - t_{m-1}$. The time instances t_i, $0 \leq i \leq M$ correspond to the time steps in a finite difference approach. We also call this decomposition the temporal mesh $\mathbb{T}_k$. By the time step m, we denote the step from t_{m-1} to t_m.

The basic domain Ω is triangulated by meshes $\mathbb{T}_h^m = \left\{\mathcal{T}_1^m, \ldots, \mathcal{T}_{M_h^m}^m\right\}$, $0 \leq m \leq M$, of qudraliteral or hexahedral elements. For our discretization, we have to assume $\mathbb{T}_h^m = \mathbb{T}_h^{m+1}$ for odd m. The sequence of the meshes in the single time steps is called $\mathbb{M}_h := (\mathbb{T}_h^m)_{m=0}^M$. The number of mesh elements in the mesh $\mathbb{T}_h^m$ is denoted by M_h^m or by M_h in the case of constant meshes.

The next step is the definition of the basis functions on the mesh elements. We begin with the spatial ones. Bi-/trilinear basis functions are used on the single elements. Together with the spatial mesh, they form the finite element space

$$V_h^m := \left\{\varphi \in \mathcal{H}^1 \,\middle|\, \forall \mathcal{T} \in \mathbb{T}_h^m : \varphi_{|\mathcal{T}} \in Q_1\left(\mathcal{T}; \mathbb{R}^d\right)\right\}.$$

Here, $Q_1\left(\mathcal{T}; \mathbb{R}^d\right)$ is the set of bi-/trilinear basis functions on a mesh cell $\mathcal{T}$.

To realise adaptive mesh refinement, we have to allow for so called hanging nodes in the discretisation, see Figure 1(a) for an illustration. Since functions from V_h^m are continuous, the basis value connected to this node is not free, but determined by the adjacent nodes. We restrict ourselves to one hanging node per edge for stability reasons. An additional property, which we assume for the mesh, is the patch structure. It is illustrated in Figure 1(b-d). We need the patch structure for the definition of the discrete Lagrange multiplier. Furthermore, it is essential in the evaluation of a posteriori error estimates, cf. [39]. We say, a mesh has patch structure, if one can always merge four/eight adjacent mesh cells to one patch element.

After the presentation of the spatial finite element spaces V_h^m, we will now discuss the trial and the test

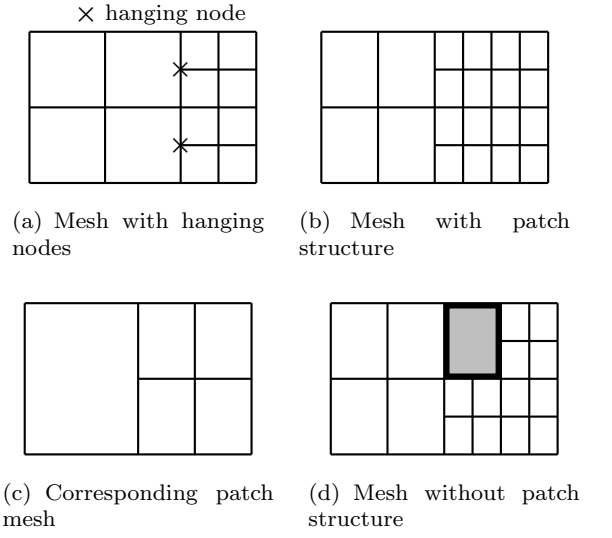

(a) Mesh with hanging nodes

(b) Mesh with patch structure

(c) Corresponding patch mesh

(d) Mesh without patch structure

Fig. 1 Graphical description of mesh properties

space for the space-time finite element method. Let us begin with the test space: It is defined as

$$W_{kh} := \left\{ \varphi \in L^2\left(I; \mathcal{H}^1\right) \,\middle|\, \begin{array}{c} \varphi_{|I_m} \in \mathcal{P}_0\left(I_m; V_h^m\right), \\ m = 1, 2, \ldots, M, \\ \varphi(0) \in V_h^0 \end{array} \right\}.$$

Here, $\mathcal{P}_q\left(\omega; X\right)$ is the linear space of polynomials on $\omega \subset \mathbb{R}$ with values in X, which have a maximum degree q. Functions from W_{kh} are piecewise constant and are possibly discontinuous at t_i, $i = 0, 1, \ldots, M$. The definition of the trial space V_{kh} is more involved, since it is difficult to ensure the global continuity, if the spaces V_h^m vary. Then hanging nodes in time arise and have to be treated in an appropriate way. A temporal hanging node is a degree of freedom, which is contained in V_h^m but not in V_h^{m-1} or vice versa. See [39] for the precise definition. We work with the approach presented in [43–45] for parabolic problems. A discussion of hanging nodes in time in the context of the wave equation is given in [46]. We use linear temporal basis functions and choose the usual Lagrange basis τ_0, τ_1 of $\mathcal{P}_1\left(I_m; \mathbb{R}\right)$. The set of the local basis functions is defined by

$$\tilde{\mathcal{P}}_1^m := \left\{\tau_i \varphi_i \,\middle|\, \varphi_i \in V_h^{m-1+i},\, i = 0, 1\right\}.$$

The space $\tilde{\mathcal{P}}_1^m$ coincides with $\mathcal{P}_1\left(I_m; V_h\right)$, if $V_h^{m-1} = V_h^m = V_h$ holds. The trial space containing globally continuous functions is given by

$$V_{kh} := \left\{ \varphi \in C\left(I; \mathcal{H}^1\right) \,\middle|\, \begin{array}{l} \varphi_{|I_m} \in \tilde{\mathcal{P}}_1^m, \\ m = 1, 2, \ldots, M \end{array} \right\}.$$

The discrete Lagrange multipliers λ_{KH} are piecewise constant in time and on the boundary mesh $\mathbb{B}_H$ representing the contact boundary Γ_C. The index H

indicates that coarser meshes may be chosen for the Lagrange multiplier in space and the index K in time, respectively. In our calculations, we use $H = 2h$ and $K = 2k$ for stability reasons. We assume that $\mathbb{T}_h$ has patch structure. Consequently, the mesh $\mathbb{B}_H$ is well defined and consists of the edges on Γ_C of the patch elements. A detailed study of this finite element approach for solving static contact problems is contained in [37]. Since M is even, the temporal patch mesh $\mathbb{T}_K := \{\mathcal{I}_1, \mathcal{I}_3, \ldots, \mathcal{I}_{M-1}\}$ with $\mathcal{I}_m = I_m \cup I_{m+1}$ is also well defined.

The spatial trial sets for the Lagrange multiplier are

$$\Lambda_{n,H}^m := \left\{\mu \in L^2(\Gamma_C) \,\middle|\, \forall \mathcal{T} \in \mathbb{B}_H^m : \mu_{|\mathcal{T}} \in \mathcal{P}_0(\mathcal{T}, \mathbb{R}_{\leq 0})\right\},$$

$$\Lambda_{t,H}^m := \left\{ \mu \in G_t \,\middle|\, \begin{array}{l} \forall \mathcal{T} \in \mathbb{B}_H^m : \mu_{|\mathcal{T}} \in \mathcal{P}_0\left(\mathcal{T}, \mathbb{R}^{d-1}\right), \\ \left|\mu_{|\mathcal{T}}\right| \leq 1 \text{ if } \mathcal{T} \subset \operatorname{supp}(s), \\ \mu_{|\mathcal{T}} = 0 \text{ if } \mathcal{T} \subset \Gamma_C \backslash \operatorname{supp}(s) \end{array} \right\},$$

$$\Lambda_H^m := \Lambda_{n,H}^m \times \Lambda_{t,H}^m.$$

We define the space-time trial sets by

$$\Lambda_{n,KH} := \left\{ \mu_n \in \tilde{\Lambda}_n \,\middle|\, \begin{array}{l} \mu_{n|\mathcal{I}_m} \in \mathcal{P}_0\left(\mathcal{I}_m; \Lambda_{n,H}^m\right), \\ m = 1, 3, \ldots, M-1 \end{array} \right\},$$

$$\Lambda_{t,KH} := \left\{ \mu_t \in \Lambda_t \,\middle|\, \begin{array}{l} \mu_{t|\mathcal{I}_m} \in \mathcal{P}_0\left(\mathcal{I}_m; \Lambda_{t,H}^m\right), \\ m = 1, 3, \ldots, M-1 \end{array} \right\},$$

$$\Lambda_{KH} := \Lambda_{n,KH} \times \Lambda_{t,KH},$$

with $\tilde{\Lambda}_n := L^2\left(I; L^2(\Gamma_C)\right)$. The discretisation reads:

Definition 3 The functions $w_{kh} \in (V_{kh} \times V_{kh})$ and $\lambda_{KH} \in \Lambda_{KH}$ with $w_{kh} = (u_{kh}, v_{kh})$ as well as $\lambda_{KH} = (\lambda_{n,KH}, \lambda_{t,KH})$ are the discrete solution of the dynamic contact problem, if and only if

$$A_{kh}(w_{kh}, \varphi_{kh}) + (b(\lambda_{KH}, \chi_{kh}, \chi_{kh})) = 0 \tag{21}$$

$$(b(\mu_{KH} - \lambda_{KH}, u_{kh} - g, \dot{u}_{kh})) \leq 0 \tag{22}$$

$$\left((\lambda_{KH}, \gamma_n(\dot{u}_{kh}))_{\Gamma_C}\right)_{I_n} = 0 \tag{23}$$

holds, where Equation (21) has to be valid for all $\varphi_{kh} = (\psi_{kh}, \chi_{kh}) \in W_{kh} \times W_{kh}$, inequality (22) for all $\mu_{KH} \in \Lambda_{KH}$, and equation (23) for all $m \in \{1, \ldots, M\}$. We call this scheme cG(1)cG(1) method. The discrete space-time bilinear form is

$$\begin{aligned} &A_{kh}(w_{kh}, \varphi_{kh}) \\ &= \sum_{m=1}^{M} \left\{ ((v_{kh} - \dot{u}_{kh}, \psi_{kh}))_{I_m} + ((\dot{v}_{kh}, \chi_{kh}))_{I_m} \right\} \\ &\quad + \sum_{m=1}^{M} \left\{ (a(u_{kh}, \chi_{kh}))_{I_m} - ((f, \chi_{kh}))_{I_m} \right\} \\ &\quad + \left(u_{kh}^0 - u_s, \chi_{kh}^0\right) + \left(v_{kh}^0 - v_s, \psi_{kh}^0\right). \end{aligned}$$

We have discretised the dynamic contact problem in the usual "finite element way". Thus, we expect as usual that the properties of the continuous solution carry over to the discrete one. In the following proposition, we discuss the conservation of the total energy:

Proposition 2 *If the right hand side f is zero, no friction occurs, and if $V_h^{m-1} \subseteq V_h^m$ for all $m \in \{0, 1, \ldots, M\}$, then the total energy is constant.*

Proof Let us assume for a moment that $V_h^{m-1} = V_h^m$ holds. Then, it is allowed to use $(\dot{v}_{kh}, \dot{u}_{kh})$ as a test function in equation (21) on a subinterval I_m and we obtain

$$\begin{aligned} 0 &= ((v_{kh}, \dot{v}_{kh}))_{I_m} + (a(u_{kh}, \dot{u}_{kh}))_{I_m} \\ &\quad + \left((\lambda_{kH}, \gamma_n(\dot{u}_{kh}))_{\Gamma_C}\right)_{I_m} \\ &= \frac{1}{2}(v_{kh}^m, v_{kh}^m) - \frac{1}{2}\left(v_{kh}^{m-1}, v_{kh}^{m-1}\right) + \frac{1}{2}a(u_{kh}^m, u_{kh}^m) \\ &\quad - \frac{1}{2}a\left(u_{kh}^{m-1}, u_{kh}^{m-1}\right) + \left((\lambda_{KH}^m, \gamma_n(\dot{u}_{kh}^m))_{\Gamma_C}\right)_{I_m}. \end{aligned}$$

Consequently, it holds

$$E_{tot}^m - E_{tot}^{m-1} = -\left((\lambda_{KH}^m, \gamma_n(\dot{u}_{kh}^m))\right)_{I_m} = 0$$

because of (23). If $V_h^{m-1} \neq V_h^m$ holds, we have to project u_{kh}^{m-1} and v_{kh}^{m-1} onto the space V_h^m. Since the projection is the identity under the assumption $V_h^{m-1} \subseteq V_h^m$, the calculation above stays valid.

4 Solution of the discrete Problem

In the last section, the space-time Galerkin was presented. It leads to a discrete problem in space and time, which has to be solved numerically. To this end, we choose the temporal test functions in such a way that the single time steps nearly decouple and we obtain a time stepping scheme similar to the Newmark scheme. Due to the fact that λ_{KH} is defined on patch elements, the discrete problems have to be solved over two time intervals.

We start with the separation of the equation defining the balance of momentum and the definition of the velocity field v. Using the test functions $(\psi_{kh}, 0)$ and $(0, \chi_{kh})$ in (21) the following system of equations arises

$$((\dot{u}_{kh} - v_{kh}, \psi_{kh})) + (u_{kh}(0) - u_s, \psi_{kh}(0)) = 0, \tag{24}$$

$$\begin{aligned} &((\dot{v}_{kh}, \chi_{kh})) + (a(u_{kh}, \chi_{kh})) - ((f, \chi_{kh})) \\ &+ (b(\lambda_{KH}, \chi_{kh}, \chi_{kh})) + (v_{kh}(0) - v_s, \chi_{kh}(0)) = 0, \end{aligned} \tag{25}$$

$$(b(\mu_{KH} - \lambda_{KH}, u_{kh} - g, \dot{u}_{kh})) \leq 0, \tag{26}$$

$$\left((\lambda_{KH}, \gamma_n(\dot{u}_{kh}))_{\Gamma_C}\right)_{I_m} = 0, \tag{27}$$

which has to hold for all $\psi_{kh}, \chi_{kh} \in W_{kh}$, all $\mu_{KH} \in \Lambda_{KH}$, and all $m \in \{1, \ldots, M\}$. We set $\varphi_{kh}^m := \varphi_{kh}(t_m)$. One possibility to choose the piecewise constant temporal basis functions of W_{kh} is the characteristic function ϕ_m on I_m with $0 \leq m \leq M$. We use $\phi_m \psi_h^m$ and $\phi_m \chi_h^m$ with ψ_h^m, $\chi_h^m \in V_h^m$ for $m = 0, 1, \ldots M$ successively as test functions in the equations (24) and (25) and obtain the time stepping scheme:

Time Stepping Scheme 1 Find $w_{kh} = (u_{kh}, v_{kh}) \in V_{kh} \times V_{kh}$ and $\lambda_{KH} = (\lambda_{n,KH}, \lambda_{t,KH}) \in \Lambda_{KH}$, where $w_{kh}^0 \in V_h^0 \times V_h^0$ is given by

$$\forall \psi_h \in V_h^0: \quad \left(u_{kh}^0 - u_s, \psi_h\right) = 0, \tag{28}$$

$$\forall \chi_h \in V_h^0: \quad \left(v_{kh}^0 - v_s, \chi_h\right) = 0. \tag{29}$$

For $m = 1, 2, \ldots, M$, $w_{kh}^m \in V_h^m \times V_h^m$ and $\lambda_{KH}^{\tilde{m}} \in \Lambda_H^{\tilde{m}}$ are the solution of the system

$$\left(u_{kh}^m - u_{kh}^{m-1}, \psi_h\right) - \frac{1}{2} k_m \left(v_{kh}^m + v_{kh}^{m-1}, \psi_h\right) = 0, \tag{30}$$

$$\left(v_{kh}^m - v_{kh}^{m-1}, \chi_h\right) + \frac{1}{2} k_m a\left(u_{kh}^m + u_{kh}^{m-1}, \chi_h\right)$$

$$+ b\left(\lambda_{KH}^{\tilde{m}}, \chi_h, \chi_h\right) - \frac{1}{2} k_m \left(f^m + f^{m-1}, \chi_h\right) = 0, \tag{31}$$

$$\left(b\left(\mu_H - \lambda_{KH}^{\tilde{m}}, u_{kh}^m - g, \dot{u}_{kh}^m\right)\right)_{I_m} \leq 0, \tag{32}$$

$$\left(\lambda_{KH}^{\tilde{m}}, \gamma_n\left(\dot{u}_{kh}^m\right)\right)_{\Gamma_C} = 0, \tag{33}$$

which has to hold for all $\psi_h, \chi_h \in V_h^m$ and all $\mu_H \in \Lambda_H^{\tilde{m}}$. Here, we set

$$\tilde{m} := \begin{cases} m, & m \text{ odd}, \\ m-1, & m \text{ even}. \end{cases}$$

All time integrals over terms only including the test and trial functions are evaluated exactly. The time integral $((f, \chi_{kh}))_m$ is approximated by the trapezoidal rule. This ensures the optimal order of convergence for the presented scheme. However, one may obtain a more accurate solution by choosing a quadrature rule of higher order like the Simpson or the two point Gauß rule. The additional error introduced by the numerical quadrature is discussed in [47]. There, continuous Galerkin methods in the context of ODEs are considered.

The equations (28) and (29) specify the discrete initial values as the spatial L^2-projection on V_h^0 of the continuous ones. Writing (30) in the form

$$\left(v_{kh}^m, \psi_h\right) = \frac{2}{k_m}\left(u_{kh}^m - u_{kh}^{m-1}, \psi_h\right) - \left(v_{kh}^{m-1}, \psi_h\right) \tag{34}$$

for all $\psi_h \in V_h^m$, we can substitute v_{kh}^m in (31) and obtain for all $\chi_h \in V_h^m$

$$\frac{2}{k_m^2}\left(u_{kh}^m, \chi_h\right) + \frac{1}{2} a\left(u_{kh}^m, \chi_h\right) + b\left(\lambda_{KH}^{\tilde{m}}, \chi_h, \chi_h\right)$$
$$= \frac{1}{2}\left(f^m + f^{m-1}, \chi_h\right) + \frac{2}{k_m^2}\left(u_{kh}^{m-1}, \chi_h\right)$$
$$+ \frac{2}{k_m}\left(v_{kh}^{m-1}, \chi_h\right) - \frac{1}{2} a\left(u_{kh}^{m-1}, \chi_h\right). \tag{35}$$

The side conditions specified in (32) and (33) read with $\Delta u_{kh}^m := u_{kh}^m - u_{kh}^{m-1}$ and $u_{kh}^{m-1/2} := 0.5\left(u_{kh}^m + u_{kh}^{m-1}\right)$

$$b\left(\mu_H - \lambda_{KH}^{\tilde{m}}, k_m\left(u_{kh}^{m-1/2} - g\right), \Delta u_{kh}^m\right) \leq 0, \tag{36}$$

$$\left(\lambda_{KH}^{\tilde{m}}, k_m^{-1} \gamma_n\left(u_{kh}^m - u_{kh}^{m-1}\right)\right)_{\Gamma_C} = 0, \tag{37}$$

for all $\mu_H \in \Lambda_H^{\tilde{m}}$. Evaluating the integrals in inequality (32) directly leads to (36), because u_{kh} is a continuous and piecewise linear function. Furthermore, the discrete persistency condition (37) is equivalent to condition (33), since all variables in (33) are constant in time.

The numerical effort for solving equation (34) is small, since it is a simple L^2-projection. If the finite element spaces V_h^m do not vary, equation (34) reduces to a simple linear combination of vectors in matrix-vector notation. The solution of the system (35-37) is more involved. If we choose $K = k$, using a Schur complement leads to a quadratic programm with nonlinear side conditions in λ_{kH}^m, c.f. [39], which is hard to solve. Thus, we use the approach presented in [3] to rewrite the side conditions such that we have only to fulfill geometrical conditions. We replace g in (36) by the function

$$\tilde{g}^m(x) := \begin{cases} \infty, & \gamma_n\left(u_{kh}^{m-1}(x)\right) < g(x) \\ \gamma_n\left(u_{kh}^{m-1}(x)\right), & \gamma_n\left(u_{kh}^{m-1}(x)\right) \geq g(x) \end{cases}.$$

This choice directly ensures (37) and the geometrical contact conditions $\gamma_n\left(u_{kh}^m\right) \leq g$ hold for $k \to 0$. Consequently we have to solve a quasi static frictional contact problem in each time step. This is done with the techniques presented in [37,38], where Coulomb's law of friction is included by a fixpoint method. Furthermore, we obtain the existence and uniqueness of the discrete solution (w_{kh}, λ_{kH}) from the static theory, provided the friction law satisfies several assumptions, c.f., e.g., [37].

However, we have to solve the system (35-37) on patch elements $\mathcal{I}_m$ in time. To obtain an efficient solution algorithm for this problem, we firstly weaken condition (37). We require the persistency condition not over the single time intervals but over the patch elements:

$$\begin{aligned} 0 &= \left(\left(\lambda_{KH}, \gamma_n\left(\dot{u}_{kh}\right)\right)_{\Gamma_C}\right)_{\mathcal{I}_m} \\ &= \left(\lambda_{KH}^m, \gamma_n\left(u_{kh}^m - u_{kh}^{m-1}\right)\right)_{\Gamma_C} \\ &\quad + \left(\lambda_{KH}^m, \gamma_n\left(u_{kh}^{m+1} - u_{kh}^m\right)\right)_{\Gamma_C} \\ &= \left(\lambda_{KH}^m, \gamma_n\left(u_{kh}^{m+1} - u_{kh}^{m-1}\right)\right)_{\Gamma_C}. \end{aligned} \tag{38}$$

Thus, we replace the requirement

$$\gamma_n\left(k_{m+1} u_{kh}^{m+1/2} + k_m u_{kh}^{m-1/2}\right) - \left(k_m + k_{m+1}\right) g \leq 0$$

by $\gamma_n\left(u_{kh}^{m+1}\right) \leq \tilde{g}^m$ using the ideas presented above for $K = k$. This approach ensures the percistency condition (38) and with it the energy conservation on $\mathcal{I}_m$. The frictional condition should also hold in the temporal integral mean value. Altogether, we have to solve the following problem for $m = 1, 3, \ldots, M-1$:

Problem 1 Find $w_{kh}^m, w_{kh}^{m+1} \in V_h^m \times V_h^m$ and $\lambda_{KH}^m \in \Lambda_H^m$ with

$$\begin{aligned}
(v_{kh}^m, \psi_h) &= \frac{2}{k_m}\left(u_{kh}^m - u_{kh}^{m-1}, \psi_h\right) - \left(v_{kh}^{m-1}, \psi_h\right), \\
\left(v_{kh}^{m+1}, \omega_h\right) &= \frac{2}{k_m}\left(u_{kh}^{m+1} - u_{kh}^m, \omega_h\right) - \left(v_{kh}^m, \omega_h\right), \\
c\left(u_{kh}^m, \chi_h\right) &= F^m\left(\chi_h\right) - b\left(\lambda_{KH}^m, \chi_h, \chi_h\right), \\
c\left(u_{kh}^{m+1}, \phi_h\right) &= F^{m+1}\left(\phi_h\right) - b\left(\lambda_{KH}^m, \phi_h, \phi_h\right), \\
0 &\geq b\left(\mu_H - \lambda_{KH}^m, u_{kh}^m - \tilde{g}^m, u_{kh}^{m+1} - u_{kh}^{m-1}\right).
\end{aligned}$$

for all $\psi_h \in V_h^m$, all $\omega_h \in V_h^{m+1}$, all $\chi_h \in V_h^m$, all $\phi_h \in V_h^{m+1}$, and all $\mu_H \in \Lambda_H^m$.

Here, we set

$$\begin{aligned}
c\left(u_{kh}^m, \chi_h\right) &:= \frac{2}{k_m^2}\left(u_{kh}^m, \chi_h\right) + \frac{1}{2}a\left(u_{kh}^m, \chi_h\right), \\
F^m\left(\chi_h\right) &:= \frac{1}{2}\left(f^m + f^{m-1}, \chi_h\right) + \frac{2}{k_m^2}\left(u_{kh}^{m-1}, \chi_h\right) \\
&\quad + \frac{2}{k_m}\left(v_{kh}^{m-1}, \chi_h\right) - \frac{1}{2}a\left(u_{kh}^{m-1}, \chi_h\right).
\end{aligned}$$

Using the Schur complement, Problem 1 is formulated as quadratic program in λ_{KH}^m with box constraints, which is then solved by an active set method. If the frictional resistance s depends also on $\lambda_{n,KH}^m$, we use a fixpoint method to solve the nonlinear system.

Let us briefly introduce the discrete optimization problem for $m = 1, 3, \ldots, M-1$. Here, we assume to ease the notations, an equidistant temporal mesh and a constant spatial mesh. Let $\underline{\mathrm{M}}$ be the usual mass matrix and $\underline{\mathrm{K}}$ the usual stiffness matrix, $\underline{\mathrm{A}} := \frac{2}{k}\underline{\mathrm{M}} + \frac{1}{2}\underline{\mathrm{K}}$, $\underline{\mathrm{D}} := \frac{6}{k}\underline{\mathrm{M}} - \frac{1}{2}\underline{\mathrm{K}}$. If k is sufficiently small, all matrices are symmetric and positive definite. Furthermore, the normal contact conditions are represented by the matrix $\underline{\mathrm{N}}$ and the tangential ones by $\underline{\mathrm{T}}$, $\underline{\mathrm{B}}^\top := \left(\underline{\mathrm{N}}^\top, \underline{\mathrm{T}}^\top\right)$. We define

$$\begin{aligned}
\underline{\mathrm{G}}_1 &:= \frac{1}{2}\left(\underline{\mathrm{f}}^{m+1} + \underline{\mathrm{f}}^m\right) - \frac{4}{k^2}\underline{\mathrm{M}}\underline{\mathrm{u}}^{m-1} - \frac{2}{k}\underline{\mathrm{M}}\underline{\mathrm{v}}^{m-1}, \\
\underline{\mathrm{G}}_2 &:= \frac{1}{2}\left(\underline{\mathrm{f}}^m + \underline{\mathrm{f}}^{m-1}\right) + \frac{2}{k^2}\underline{\mathrm{M}}\underline{\mathrm{u}}^{m-1} + \frac{2}{k}\underline{\mathrm{M}}\underline{\mathrm{v}}^{m-1} \\
&\quad - \frac{1}{2}\underline{\mathrm{K}}\underline{\mathrm{u}}^{m-1}, \\
\underline{\mathrm{G}} &:= \underline{\mathrm{A}}^{-1}\underline{\mathrm{G}}_1 + \underline{\mathrm{A}}^{-1}\underline{\mathrm{D}}\underline{\mathrm{A}}^{-1}\underline{\mathrm{G}}_2 - \underline{\tilde{\mathrm{g}}}^{m+1}, \\
\underline{\mathrm{Q}} &:= \underline{\mathrm{B}}\underline{\mathrm{A}}^{-1}\left(\underline{\mathrm{I}} + \underline{\mathrm{D}}\underline{\mathrm{A}}^{-1}\right)\underline{\mathrm{B}}^\top.
\end{aligned}$$

Here, underlined characters represent the vectors corresponding to the discrete functions. Then $\underline{\lambda}^m$ is the solution of the quadratic program

$$\begin{aligned}
&\min_{\underline{\mu}} \underline{\mu}^\top \underline{\mathrm{Q}}\underline{\mu} - \underline{\mu}^\top \underline{\mathrm{G}} \\
&\text{s. t. } \underline{\mu}_n^m \leq 0,\ -\underline{\mathrm{s}}^m \leq \underline{\mu}_t^m \leq \underline{\mathrm{s}}^m.
\end{aligned}$$

5 Stability analysis

We have presented a mixed space time finite element discretization of dynamic contact problems. It is well known that ensuring stability of the approach is crucial for this type of discretization. In this section, we discuss stability for the presented approach. The section is divided into two parts. In this first one, the stability in time is discussed. Then we focus on stability in space and time.

5.1 Stability in time

To analyse the stability in time, we consider the following example, which is a 2d version of an example given in [5]: The domain is $\Omega := [-h_0 - L, -h_0] \times [0, 2]$, $h_0 = 5$, $L = 10$, and the time interval $I = [0, 1.5]$. We choose $E = 900$, $\nu = 0$, and $\rho \equiv 1$. The possible contact boundary is given by $\Gamma_C = \{-5\} \times [0, 2]$ and we set $\Gamma_D = \emptyset$ as well as $\Gamma_N = \partial\Omega \backslash \Gamma_C$. The initial conditions are $u_s \equiv 0$ and $v_s \equiv (v_0, 0)^\top$, $v_0 = 10$. The rigid foundation is given by $g \equiv 0$ and we set $s = 0$. From the specific velocity $c_0 = \sqrt{E/\rho} = 30$, we can calculate the time $\tau_w = v_0/c_0 = 1/3$, which a stress wave needs to travel through Ω from $x = -5$ to $x = -15$. The impact time is $t_1 = 5/10 = 0.5$ and the time for loosing contact is $t_2 = t_1 + 2\tau_w = 7/6$. With these values we can state the analytical solution of this problem: It holds for the displacement $u := (u_1, 0)$ with

$$u_1(x_1, x_2, t) := \begin{cases} v_0 t, & t \leq t_1, \\ h_0 + v_0\omega(x_1, t), & t_1 < t \leq t_2, \\ h_0 - v_0\left(t - t_2\right), & t_2 < t \end{cases}$$

and

$$\begin{aligned}
\omega(x_1, t) &:= \min\left\{\omega_x(x_1), \omega_t(t)\right\}, \\
\omega_x(x_1) &:= -\frac{h_0 + x_1}{c_0}, \\
\omega_t(t) &:= \tau_w - \left|t - t_1 - \tau_w\right|,
\end{aligned}$$

for the velocity $v := (v_1, 0)$ with

$$v_1\left(x_1, x_2, t\right) := \begin{cases} v_0, & t \leq t_1, \\ -v_0\Phi(x_1, t), & t_1 < t \leq t_2, \\ -v_0, & t_2 < t, \end{cases}$$

and

$$\Phi(x_1, t) := \begin{cases} 0, & \omega_x(x_1) \leq \omega_t(t)|, \\ \operatorname{sign}\left(t - t_1 - \tau_w\right), & \omega_x(x_1) > \omega_t(t), \end{cases}$$

as well as for the normal contact stress

$$\sigma_{nn}\left(t\right) = \lambda\left(t\right) = \begin{cases} 0, & t \notin [t_1, t_2], \\ -\frac{Ev_0}{c_0} = -300, & \text{else.} \end{cases} \tag{39}$$

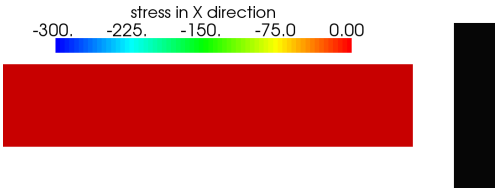

(a) $t = 0.4$

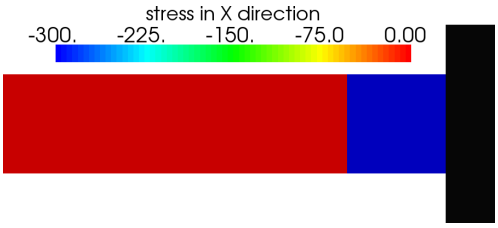

(b) $t = 0.6$

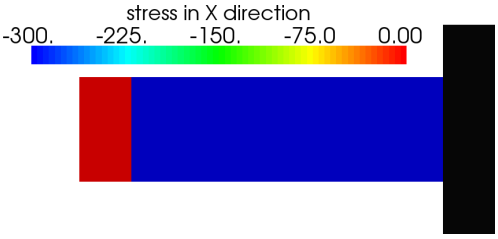

(c) $t = 0.8$

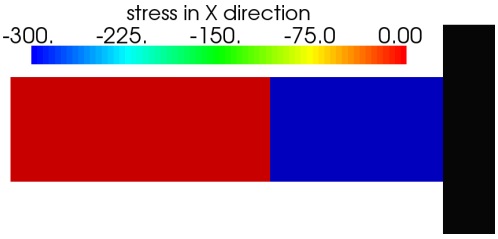

(d) $t = 1$

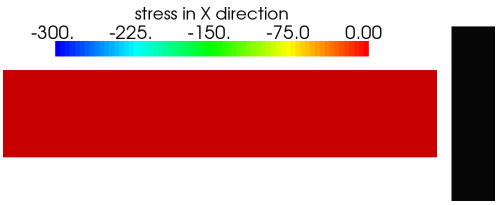

(e) $t = 1.2$

Fig. 2 Analytic stress distribution in Ω for different time instances

The analytical solution is illustrated in Figure 2. We use it in Section 6.1 to analyse the spatial and temporal convergence rate of the proposed method. Here, we focus on the stability of λ_{KH}.

Equation (39) shows that λ does not depend on x and thus λ_{KH} also does not. Consequently, it is sufficient to consider the temporal development of λ_{kH} only. In Figure 3(a), λ_{kH} is depicted for $K = k = 0.01$ and obviously shows an unstable behaviour. This is not surprising, because we know for the static case that the combination of linear trial functions for the displacement and piecewise constant basis functions for the Lagrange multiplier on the same mesh leads to unstable discretizations, c.f. [37]. It should be remarked that a projection of λ_{kH} onto Λ_{2kH} leads to a reasonable approximation of λ, c.f. Figure 3(b).

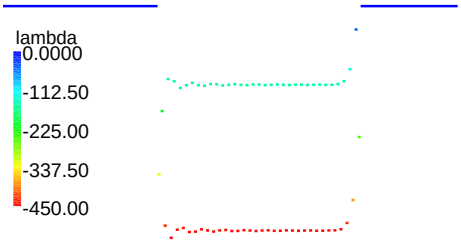

(a) Plot of λ_{KH} for the cG(1)cG(1) method with $K = k$

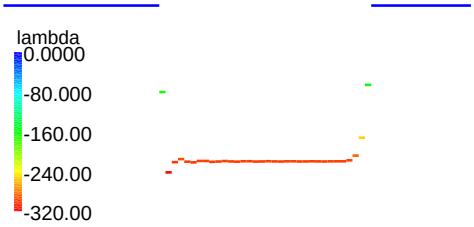

(b) Plot of the projection of λ_{kH} on Λ_{2kH}

Fig. 3 Plot of λ_{KH} for the cG(1)cG(1) method with $K = k$

In Figure 4, λ_{KH} is plotted for different k with $K = 2k$. For $k = 0.01$ and $k = 0.005$, we observe stable behaviour, but not for $k = 0.0025$. If we vary the spatial mesh width H, we observe that the stability limit also changes, it decreases linearly with H. Studying also other examples, we come to the conclusion that a CFL-type condition connecting the temporal and the spatial discretization of the form

$$\frac{H}{K} \leq c_0 \tag{40}$$

has to hold to ensure stability.

Since the stabilization by choosing $K = 2k$ leads to a complex discrete problem and we have in addition to ensure (40), we also consider other ways to stabilize the discretization. The first idea is to integrate equation (30) numerically by the right box rule. This leads to

$$v_{kh}^m = \frac{1}{k}\left(u_{kh}^m - u_{kh}^{m-1}\right)$$

instead of (34). Since v_{kh}^m does not depend on v_{kh}^{m-1} anymore, the oscillations in v_{kh} are removed and a stable discretization scheme arises, c.f. Figure 5(a). It corresponds to the cG(1)dG(0) scheme, where piecewise constant and discontinuous trial functions in time are used

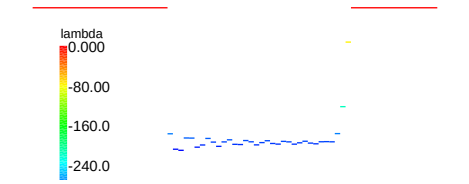

(a) $k = 0.01$

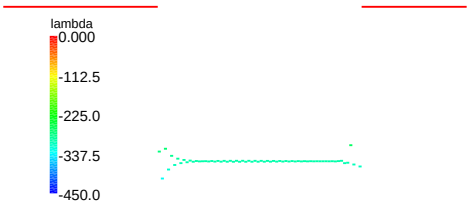

(b) $k = 0.005$

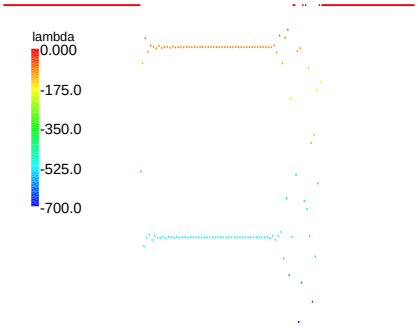

(c) $k = 0.0025$

Fig. 4 Plot of λ_{KH} for different k with $K = 2k$

for the velocity. Unfortunately, the cG(1)dG(0) method is strongly numerically dissipative and converges only of first order in time.

Another approach to stabilize the discretization is based on the redistribution of the mass in the mass matrix, c.f. [14,15]. It decouples the boundary nodes in the contact zone from the acceleration. The modified mass matrix can efficiently be computed by quadrature rules for linear basis functions in space. But the construction in three dimension and for higher order trial functions is difficult. However, this method ensures the conservation of energy. The Lagrange multiplier λ_{KH} of this approach is depicted in Figure 5(b). In the following, we name this scheme "reduced integration" or simply "reduced".

The last approach for stabilization, is based on the ideas in [18]. There the predicted displacement $u^m_{\text{pred}} := u^{m-1}_{kh} + k_m v^{m-1}_{kh}$ in the Newmark method is projected onto the addmissible set K^m_h, i.e.

$$\left(u^m_{\text{pred}}, \varphi - u^m_{\text{pred}}\right) \geq \left(u^{m-1}_{kh} + k_m v^{m-1}_{kh}, \varphi - u^m_{\text{pred}}\right)$$

(a) cG(1)dG(0) method

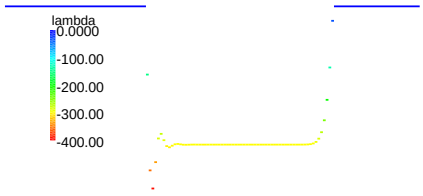

(b) Redistributed mass matrix

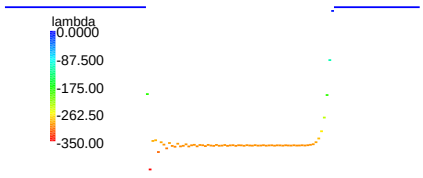

(c) Velocity projection

Fig. 5 Plot of λ_{KH} for different ways to stabilize the method with $K = k = 0.01$

for all $\varphi \in K^m_h$. We do not introduce u^m_{pred} into the calculation, but ensure $u^{m+1}_{\text{pred}} \in K^m_h$ by projecting v^m_{kh} onto the set

$$\tilde{K}^m_h := \left\{ v_h \in V^m_h \,\middle|\, \begin{array}{l} \gamma_n\left(v_h\right)(x) \leq 0,\ x \in \Gamma_C \\ \text{if } \gamma_n\left(u^m_{kh}\right)(x) \geq g(x) \end{array} \right\}.$$

Consequently, we replace (34) by

$$\left(v^m_{kh}, \varphi - v^m_{kh}\right) \geq \left(\frac{2}{k_m}\left(u^m_{kh} - u^{m-1}_{kh}\right) - v^{m-1}_{kh}, \varphi - v^m_{kh}\right) \quad (41)$$

for all $\varphi \in \tilde{K}^m_h$. This idea leads to a stable discretization scheme, see Figure 5(c). But it is weakly energy dissipative and we have additionally to solve (41), which can be performed locally. We refer to this scheme by "projection".

5.2 Stability in space

To investigate the stability in space, we consider the following example: The domain Ω is given by $\Omega = [-2, 0] \times [0, 2]$ and $I = [0, 0.1]$. The contact boundary is $\Gamma_C = \{0\} \times [0, 2]$. We prescribe inhomogeneous Neumann boundary conditions

$$q_n(x,t) := \begin{cases} \left(-10x_2^2 + 20x_2, 0\right)^\top, & x \in \Gamma_{N_1},\ t < 0.01 \\ 0, & \text{else,} \end{cases}$$

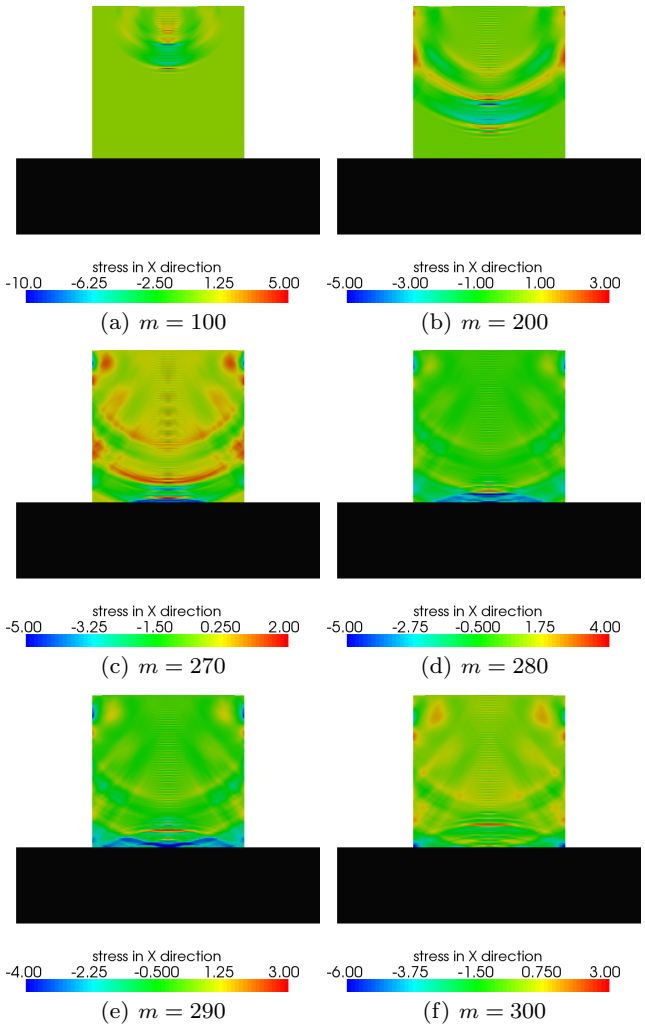

Fig. 6 Plot of the numerical solution for the cG(1)cG(1) scheme, $M = 400$ and $M_h = 20480$.

on $\Gamma_N = \partial\Omega \backslash \Gamma_C = \Gamma_{N_1} \cup \Gamma_{N_2}$ with $\Gamma_{N_1} := \{-2\} \times [0.875, 1.125]$ and $\Gamma_{N_2} = \Gamma_N \backslash \Gamma_{N_1}$. As above, we choose $E = 900$, $\nu = 0$, $\rho \equiv 1$, $s = 0$, and $g \equiv 0$. A numerical solution for this example is depicted in Figure 6. We observe a stress wave emerging from the inhomogeneous Neumann boundary conditions on Γ_{N_1}, which hits the obstacle in the middle of Γ_C, goes towards the boundary, and is reflected.

We exemplarily investigate the cG(1)cG(1) method in this section. The results directly carry over to the other schemes. In Figure 7 a plot of $\lambda_{n,KH}$ is depicted for $H = 2h$. The results correspond to the observations in the displacement, c.f. Figure 6. To investigate the stability in space, we have a detailed look on single time steps. In Figure 8, $\lambda^m_{n,KH}$ is plotted for different time steps m and $H = 2h$ as well as $H = h$. The arising instablilities for $H = h$ are obvious.

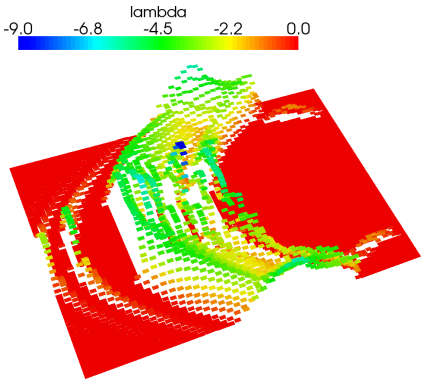

Fig. 7 Plot of the Lagrange multiplier for the cG(1)cG(1) scheme, $M = 400$, $M_h = 20480$, $K = 2k$, and $H = 2h$.

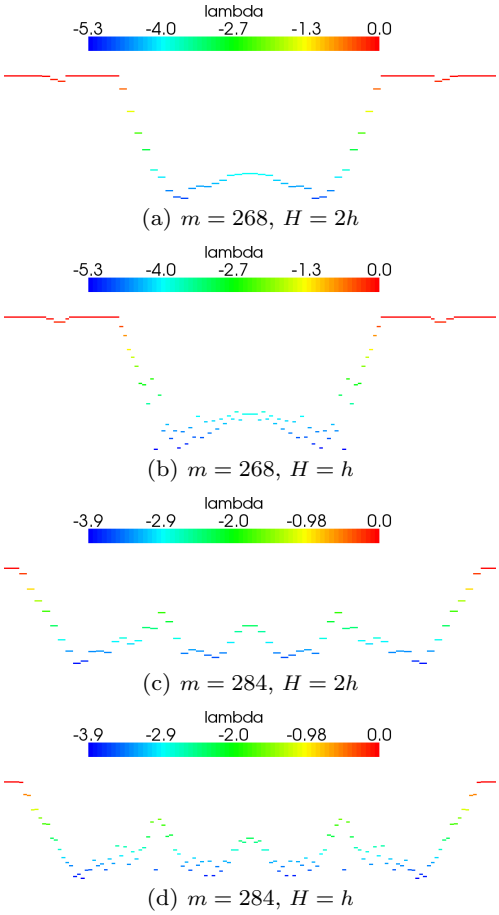

Fig. 8 Plot of the Lagrange multiplier in single time steps for the cG(1)cG(1) scheme, $M = 400$, $M_h = 20480$, and $K = 2k$.

6 Numerical results

Two illustrative examples are considered in this section. The goal is to provide a good insight into the methods and to compare their properties. Therefore, we have choosen simpler examples to ease the discussion and to exclude some minor effects.

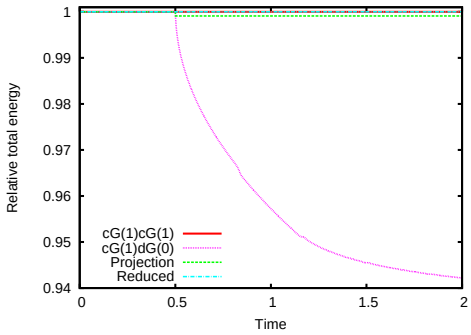

(a) Energy loss over time t for $M = 3200$ and $M_h = 20480$

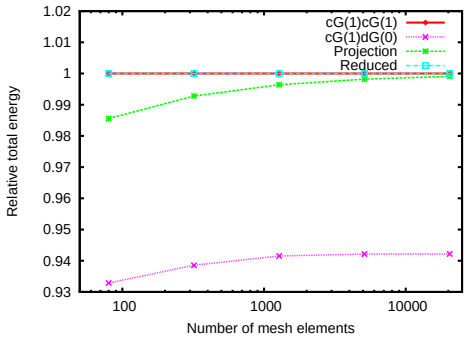

(b) Energy loss w.r.t to h, $M = 3200$

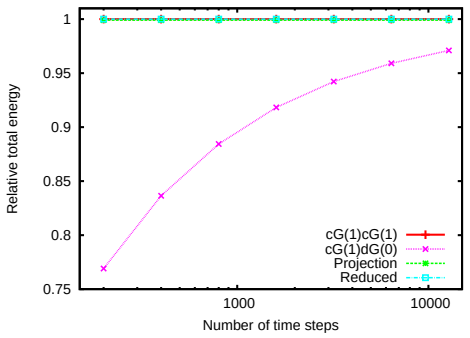

(c) Energy loss w.r.t. to k, $M_h = 20480$

Fig. 9 Comparison of the energy loss for the four different schemes.

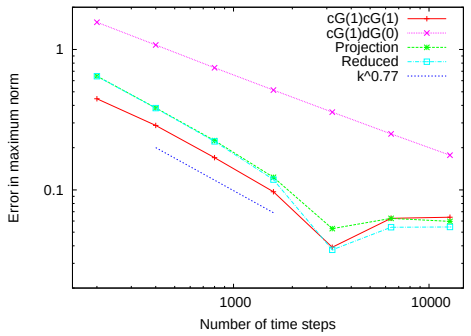

(a) Convergence w.r.t. k for $M_h = 20480$

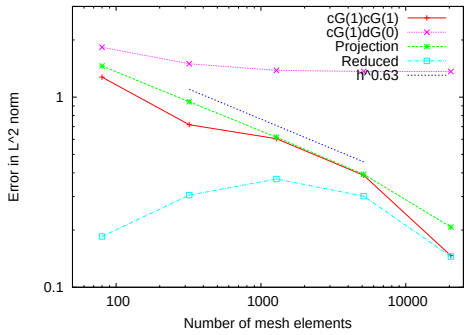

(b) Convergence in the L^2-norm w.r.t. h for $M = 3200$

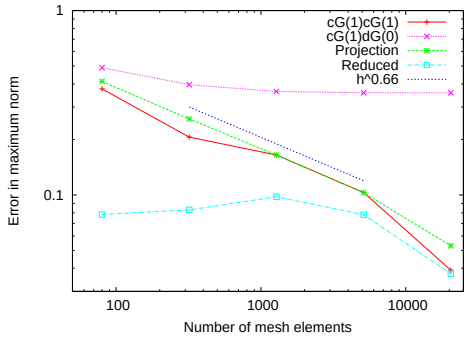

(c) Convergence in the L^∞-norm w.r.t. h for $M = 3200$

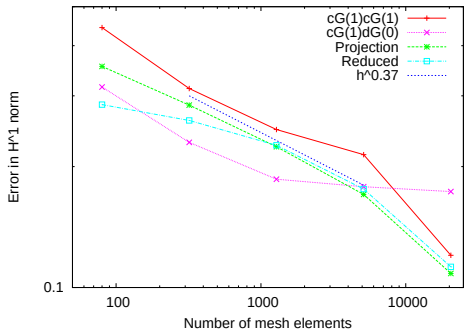

(d) Convergence in the H^1-norm w.r.t. h for $M = 3200$

Fig. 10 Comparison of the convergence behaviour for the four different methods.

6.1 Frictionless bar impact

Here, we take the example from Section 5.1 up again to discuss the accuracy of the presented methods and the issue of energy conservation. In Figure 9(a), the developement of the energy for the four different discussed schemes is plotted. We observe energy conservation as expected for the cG(1)cG(1) and the reduced integration method. In the scheme stabilized with an additional projection, we loose a small amount of energy during the first contact and then the energy is conserved. The numerical dissipativity of the cG(1)dG(0) is clear to see and we loose a lot of energy. In the Fig-

ures 9(b) and 9(c), the lost energy during the whole calculation is compared for the four different schemes w.r.t. to the spatial mesh width h and the time step length k. We find that the cG(1)cG(1) and the reduced integration method are energy conserving for all h and k. In this example, the lost energy of the projection scheme only depends on h and converges of order h. In more complex examples, we also observe an dependence on k. For the cG(1)dG(0) method, we notice a strong dependence on the time step length k. Especially for large time steps, the loss of more than 20 % of energy is not acceptable.

The convergence behaviour of the four different methods are illustrated in Figure 10. W.r.t. the time step length k, we observe that the cG(1)cG(1), the reduced integration, and the projection method all converge of order $\mathcal{O}\left(k^{0.77}\right)$ and that the error is about the same size, see Figure 10(a). For unconstrained and sufficiently smooth problems, these methods obtain a convergence rate $\mathcal{O}\left(k^2\right)$, which is reduced due to the missing regularity here. In comparison to the predicted consistency of order $\mathcal{O}\left(k^{0.5}\right)$ for the stabilized Newmark method in [21], we observe here a faster convergence. The cG(1)-dG(0) method lead to a considerably larger error and a smaller convergence rate.

Concerning the convergence w.r.t. to h, we have to divide three different behaviours. The cG(1)cG(1) and the projection scheme behave similar. We observe a convergence rate of $\mathcal{O}\left(h^{0.63}\right)$ for the L^2-norm, $\mathcal{O}\left(h^{0.66}\right)$ for the L^∞-norm, and $\mathcal{O}\left(h^{0.37}\right)$ for the H^1-norm, see Figures 10(b), 10(c), and 10(d). The rates are reduced in comparison to the smooth and unconstrained case, where we obtain $\mathcal{O}\left(h^2\right)$ in the L^2-norm, $\mathcal{O}\left(h^2 \log h\right)$ in the L^∞-norm, and $\mathcal{O}\left(h\right)$ in the H^1-norm. The reason is the missing regularity of this example. For the cG(1)dG(0) scheme, we obtain no clear results, beacuse the slow convergence w.r.t. k falsifies the measured errors. The reduced integration method shows a somehow strange behvaiour. We observe small errors in the L^2- and the L^∞-norm for large h, which then slightly grow and finally decrease to a similar amount compared with the cG(1)cG(1) and the projection method. Consequently, it is impossible to calculate a convergence rate. In the H^1-norm, we have a similar behaviour, but the error is monotonely decreasing.

6.2 Bar impact with friction

In this section, we investigate an example with friction. The domain is $\Omega = [-4,-1] \times [-6,-1]$, $\Gamma_D = \emptyset$, $\Gamma_C = [-4,-1] \times \{-1\}$, and $I = [0, 0.4]$. We assume homogeneous Neumann boundary conditions on $\Gamma_N = \partial\Omega \backslash \Gamma_C$. The obstacle is parametrised by the function

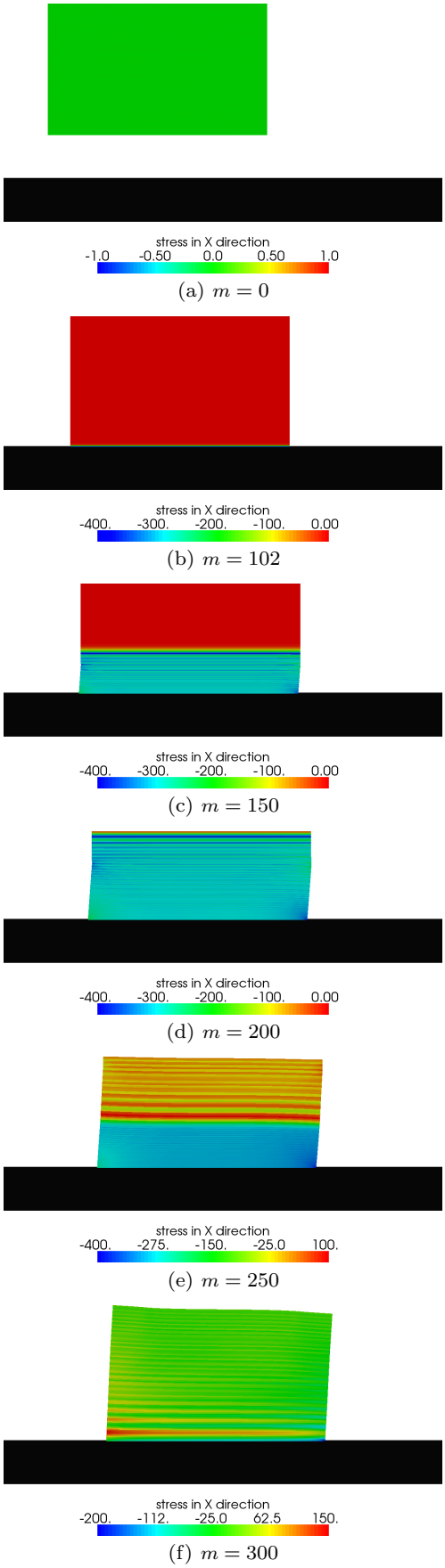

Fig. 11 Plot of the numerical solution for the cG(1)cG(1) scheme, $M = 400$ and $M_h = 15360$.

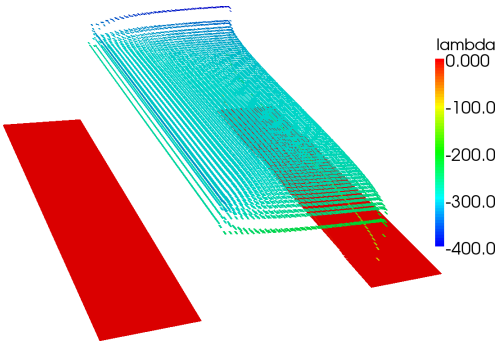

(a) Plot of $\lambda_{n,KH}$ for the cG(1)cG(1) scheme, $M = 400$, and $M_h = 15360$

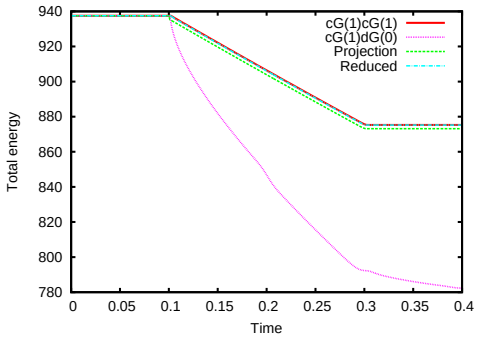

(b) Plot of the total energy for $M = 400$, and $M_h = 15360$

Fig. 12 Plot of the Lagrange multiplier for the cG(1)cG(1) scheme and of the energy developement.

$g = 0$. We set the material properties to $E = 900$, $\nu = 0$, and $\rho \equiv 1$. The initial conditions are $u_s \equiv 0$ and $v_s \equiv (10, 5)^\top$. We consider Coulomb type friction with $\mathcal{F} = 0.05$. In Figure 11, the numerical solution is illustrated. The stable Lagrange multiplier is plotted in Figure 12(a).

In the last section, we have discussed energy conservation in the context of frictionless contact. During frictional contact, energy is dissipated. What we observe here is that the cG(1)cG(1) and the reduced integration method lead to the same energy curve as well as that the curve of the projection scheme is almost parallel, we only have an additional dissipation of energy in the time step of first contact, c.f. Figure 12(b). The amount of energy dissipated during the calculation by the cG(1)cG(1) and the reduced integration method is equal to the energy dissipated by friction, which can be calculated from $\lambda_{t,KH}$ and $\dot{u}$. We find here again the strong numerical dissipaty of the cG(1)dG(0) method. The developement of the loss of energy due to numerical reasons behaves exactly the same way as in the frictionless example.

7 Conclusions and outlook

A space-time finite element method to discretize dynamic frictional contact problems have been presented. The crucial point is to ensure the stability of the presented scheme, i.e. to circumvent oscillations in the Lagrange multipliers. Four different methods have been discussed and while all ensure the stability of the proposed ansatz, the cG(1)dG(0) method lead to less effective discretizations and is strongly energy dissipative. The other three methods lead to reasonable results. As already mentioned in the introduction, the space-time finite element discretization can serve as basis for developing a posteriori error estimates w.r.t. nonlinear functionals of interest, c.f. [39]. However, the space-time formulation should also provide the opportunity to derive a rigorous mathematical proof of stability and convergence.

The presented discretization scheme can also be extended to more complex problems. Here, we think of the inclusion of nonlinear material laws with finite deformations. Furthermore, coupled thermomechanical contact problems are an interesting topic of research and the presented approach should be applicable. A second interesting topic is the extension to higher order finite elements. In space, the extension can be carried out with the ideas presented in [38]. The temporal variable is much more involved, since the solution of the discrete problems and the formulation of the contact conditions is difficult.

Acknowledgments

This research work was supported by the Deutsche Forschungsgemeinschaft (DFG) within the Priority Program 1480, Modeling, Simulation, and Compensation of Thermal Effects for Complex Machining Processes, in the grant BL 256/11-1.

References

1. Weinert K, Blum H, Jansen T, Rademacher A (2007) Simulation based optimization of the NC-shape grinding process with toroid grinding wheels. Prod Eng 1(3):245-252
2. Kikuchi N, Oden J T (1988) Contact Problems in Elasticity: A Study of Variational Inequalities and Finite Element Methods. SIAM, Studies in Applied Mathematics
3. Laursen T A (2002) Computational Contact and Impact Mechanics. Springer, Berlin
4. Wriggers P (2002) Computational Contact Mechanics. John Wiley & Sons Ltd, Chichester
5. Doyen D, Ern A, Piperno S (2011) Time-Integration Schemes for the Finite Element Dynamic Signorini Problem. SIAM J Sci Comput 33:223-249

6. Krause R, Walloth M (2009) Presentation and Comparison of Selected Algorithms for Dynamic Contact Based on the Newmark Scheme. ICS Preprint 2009-08, Institute of Computational Science, Universita della Svizzera Italiana
7. Newmark N M (1959) A Method of Computation for Structural Dynamics. Journal of the Engineering Mechanics Division ASCE 85(EM3):67-94
8. Chung J, Hulbert, G M (1993) A Time Integration Algorithm for Structural Dynamics with Improved Numerical Dissipation: The Generalized-α Method. J Appl Mec. 60:371-375
9. Talaslidis D, Panagiotopoulos P D (1982) A Linear Finite Element Approach to the Solution of the Variational Inequalities arising in Contact Problems of Structural Dynamics. Int J Numer Methods Eng 18:1505-1520
10. Bathe K J, Chaudhary A B (1986) A Solution Method for Static and Dynamic Analysis of Three-Dimensional Contact Problems with Friction. Comput Struct 24(6):855-873
11. Czekanski A, El-Abbasi N, Meguid S A (2001) Optimal Time Integration Parameters for Elastodynamic Contact Problems. Commun Numer Math Engrg 17:379-384
12. Armero F, Petőcz E (1998) Formulation and analysis of conserving algorithms for frictionless dynamic contact/impact problems. Comput Methods Appl Mech Eng 158:269-300
13. Laursen T A, Chawla V (1997) Design of Energy Conserving Algorithms for Frictionless Dynamic Contact Problems. Int J Numer Methods Eng 40:863-886
14. Khenous H B, Laborde P, Renard Y (2008) Mass redistribution method for finite element contact problems in elastodynamics. Eur J Mech A Solids 27(5):918-932
15. Hager C, Hüeber S, Wohlmuth B I (2008) A Stable Energy Conserving Approach for Frictional Contact Problems based on Quadrature Formulas.Int J Numer Methods Eng 73:205-225
16. Kane C, Repetto E A, Ortiz M, Marsden J E (1999) Finite Element Analysis of nonsmooth contact. Comput Methods Appl Mech Eng 180:1-26
17. Pandolfi A, Kane C, Marsden J E, Ortiz M (2002) Time-discretized variational formulation of non-smooth frictional contact. Int J Numer Methods Eng 53:1801-1829
18. Deuflhard P, Krause R, Ertel S (2007) A contact-stabilized Newmark method for dynamical contact problems. Int J Numer Methods Eng 73(9):1274-1290
19. Krause R, Walloth M (2009) A time discretization scheme based on Rothe's method for dynamical contact problems with friction. Comput Methods Appl Mech Eng 199(1-4):1-19
20. Klapproth C, Deuflhard P, Schiela A (2009) A Perturbation Result for Dynamical Contact Problems. Numer Math Theor Meth Appl 2(3):237-257
21. Klapproth C, Schiela A, Deuflhard P (2010) Consistency Results for the contact-stabilized Newmark Method Numer Math 116(1): 65-94
22. Klapproth C, Schiela A, Deuflhard P (2011) Adaptive Timestep Control for the Contact-Stabilized Newmark Method Numer Math 119(1):49-81
23. Blum H, Rademacher A, Schröder A (2008) Space adaptive finite element methods for dynamic obstacle problems. ETNA, Electron Trans Numer Anal 32:162-172
24. Blum H, Rademacher A, Schröder A (2009) Space adaptive finite element methods for dynamic Signorini problems. Comput Mech 44(4):481-491
25. Wriggers P, Vu Van T, Stein E (1990) Finite Element Formulation of Large Deformation Impact-Contact Problems with Friction. Comput Struct 37(3):319-331
26. McDevitt T W, Laursen T A (2000) A Mortar-Finite Element Formulation for Frictional Contact Problems. Int J Numer Methods Eng 48(10):1525-1547
27. Puso M, Laursen T A (2002) A 3D Contact Smoothing Method using Gregory Patches. Int J Numer Methods Eng 54(8):1161-1194
28. Dickopf T, Krause R (2009) Efficient simulation of multibody contact problems on complex geometries: A flexible decomposition approach using constrained minimization. Int J Numer Methods Eng 77(13):1834-1862
29. Hüeber S, Matei A, Wohlmuth B I (2007) Efficient algorithms for problems with friction. SIAM J Sci Comput 29(1):70-92
30. Hüeber S,d Stadler G, Wohlmuth B I (2008) A primal-dual active set algorithm for three-dimensional contact problems with Coulomb friction. SIAM J Sci Comput 30(2):572-596
31. Kornhuber R, Krause R (2001) Adaptive multigrid methods for Signorini's problem in linear elasticity. Comput Vis Sci 4(1):9-20
32. Wohlmuth B I, Krause R (2003) Monotone multigrid methods on nonmatching grids for nonlinear multibody contact problems. SIAM J Sci Comput 25 (1):324-347
33. Haslinger J, Dostál Z, Kučera R (2002) On a splitting type algorithm for the numerical realization of contact problems with Coulomb friction. Comput Methods Appl Mech Eng 191(21-22):2261-2281
34. Haslinger J, Sassi T (2004) Mixed finite element approximation of 3D contact problems with given friction: error analysis and numerical realization. Math Mod Numer Anal 38:563-578
35. Haslinger J, Kučera R, Dostál Z (2004) An algorithm for the numerical realization of 3D contact problems with Coulomb friction. J Comput Appl Math 164-165:387-408
36. Dostál Z, Horák D, Kučera R, Vondrák V, Haslinger J, Dobiáš J, Pták S (2005) FETI based algorithms for contact problems: Scalability, large displacements and 3D Coulomb friction. Comput Methods Appl Mech Eng 194(2-5):395-409
37. Schröder A, Blum H, Rademacher A, Kleemann H (2011) Mixed FEM of higher order for contact Problems with friction. J Numer Anal Model 8(2):302-323
38. Blum H, Kleemann H, Rademacher A, Schröder A (2008) On solving frictional contact problems part II: Dynamic case. Ergebnisberichte des Instituts für Angewandte Mathematik, Technische Universität Dortmund, ISSN 2190-1767, No 378
39. Rademacher A (2010) Adaptive Finite Element Methods for Nonlinear Hyperbolic Problems of Second Order. Dissertation, Fakultät für Mathematik, Technische Universität Dortmund, Verlag Dr. Hut, avaible online: https://eldorado.tu-dortmund.de/handle/2003/27214
40. Evans L C (1998) Partial Differential Equations, American Mathematical Society, Providence
41. Ahn J, Stewart D E (2009) Dynamic frictionless contact in linear viscoelasticity. IMA J Numer Anal 1:43-71
42. Papadopoulos P, Taylor R L (1993) On a Finite Element Method for Dynamic Contact/Impact Problems. Int J Numer Methods Eng 36:2123-2140
43. Becker R (2001) Adaptive Finite Elements for Optimal Control Problems. Habilitation thesis, Ruprecht-Karls-Universität Heidelberg
44. Meidner D (2008) Adaptive Space-Time Finite Element Methods for Optimization Problems Governed by Nonlinear Parabolic Systems. Dissertation, Ruprecht-Karls-Universität Heidelberg

45. Schmich M, Vexler B (2008) Adaptivity with dynamic meshes for space-time finite element discretizations of parabolic equations. SIAM J Sci Comput 30:369-393
46. Bangerth, W (1998) Adaptive Finite-Elemente-Methoden zur Lösung der Wellengleichung mit Anwendung in der Physik der Sonne. Diploma thesis, Ruprecht-Karls-Universität Heidelberg
47. Logg A (2006) Multi-Adaptive Galerkin Methods for ODEs III: A priori error estimates. SIAM J Numer Anal 43(6):2624-2646